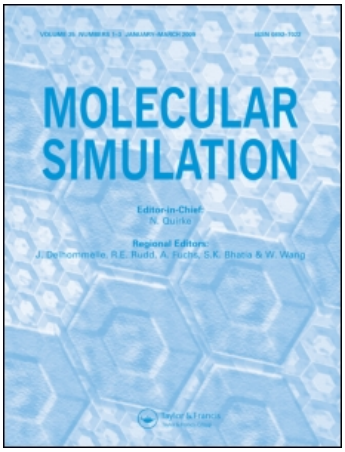

Molecular Simulation

Publication details, including instructions for authors and subscription information:
http://www.informaworld.com/smpp/title~content=t713644482

Binding mode analysis between membrane dipeptidase and its substrates

M. Kim[a]; J. Kim[a]; E. Jung[a]; K. Choi[b]; J. -M. Shin[c]; S. -K. Kang[d]; M. -K. Kim[d]; Y. -J. Choi[d]; S. -H. Choi[a]
[a] Insilicotech Co. Ltd, Seoul, South Korea [b] Department of Chemistry, Korea University, Seoul, South Korea [c] SBScience Co. Ltd, Seoul, South Korea [d] School of Agriculture Biotechnology, Seoul National University, Seoul, South Korea

To cite this Article Kim, M. , Kim, J. , Jung, E. , Choi, K. , Shin, J. -M. , Kang, S. -K. , Kim, M. -K. , Choi, Y. -J. and Choi, S. -H.(2007) 'Binding mode analysis between membrane dipeptidase and its substrates', Molecular Simulation, 33: 6, 495 — 503

To link to this Article: DOI: 10.1080/08927020701236763

URL: http://dx.doi.org/10.1080/08927020701236763

Molecular Simulation, Vol. 33, No. 6, May 2007, 495–503

Taylor & Francis
Taylor & Francis Group

Binding mode analysis between membrane dipeptidase and its substrates

M. KIM†, J. KIM†, E. JUNG†, K. CHOI‡, J. -M. SHIN¶, S. -K. KANG§, M. -K. KIM§, Y. -J. CHOI§ and S. -H. CHOI†*

†Insilicotech Co. Ltd, A-1101, Kolontripolis, 210, Geumgok-Dong, Bundang-Gu, Seongnam-Shi, Gyeonggi-Do, Seoul 463-943, South Korea
‡Department of Chemistry, Korea University, Anam-dong, Seongbuk-Gu, Seoul 136-701, South Korea
¶SBScience Co. Ltd, 3F, Sung-Ok BD, 4-1, Sunae-Dong, Bundang-Gu, Seongnam-Shi, Gyeonggi-Do, Seoul 463-825, South Korea
§School of Agriculture Biotechnology, Seoul National University, San56-1, Shilim-Dong, Kwanak-gu, Seoul 151-742, South Korea

(Received December 2006; in final form January 2007)

Membrane dipeptidase (MDP) is a membrane-bound glycoprotein involved in the hydrolysis of dipeptides, showing specific activity for dipeptides. Recent study showed that membrane dipeptidase was the receptor for a lung-targeting peptide identified by *in vivo* phage display and the crystal structure of the cilastatin-liganded human renal dipeptidase was determined. We performed a pharmacophore-based virtual screening and molecular docking in order to characterize MDP binding interactions with its substrates. A ligand-based pharmacophore model represented only a slight enrichment because of a lacked variety and centralization of ligand features. Molecular docking study was used to incorporate ligand conformational changes in the binding sites and the performance was much better than pharmacophore model; only 10% of compound library needed to be screened in order to detect all included active compounds. In addition, we found that one of the crystallographically observed water molecules plays an important role in the binding modes between MDP and its substrate.

Keywords: Membrane dipeptidase (MDP); Cilastatin; Docking; Pharmacophore; Virtual screening

1. Introduction

Membrane dipeptidase (MDP; E.C.3.4.13.19) is located at the renal brush border membrane, lung, intestine and pancreatic zymogen granules, where it is attached by a glycosyl-phosphatidylinositol anchor [1–3]. This zinc-dependent metalloenzyme exists as a disulphide-linked homodimer of subunit mass 63 kDa in the human and catalyzes the hydrolysis of a wide range of dipeptides, including those with D-amino acids at the C-terminus [4,5]. MDP is involved in the metabolism of leukotrienes and inactivates leukotriene D4 (LTD4) by converting it to leukotriene E4 (LTE4). It also acts in the degradation of extracellular glutathione, cleaving the Cys–Gly dipeptide after glutamate has been removed by gamma-glutamyl transpeptidase. MDP is unique among mammalian peptidases in possessing β-lactamase activity toward imipenem and a number of other carbapenem antibiotics [6–9].

In recent studies, phage display libraries were used to select *in vivo* for peptides capable of homing to the vasculature of a given organ or tissue and MDP was identified as the receptor for peptides that selectively home to lung endothelium [3,10–12]. These results suggest potential applications of MDP binding molecules in the targeted drug delivery to the lungs as well as in the inhibition of dipeptide and β-lactam degradations.

The 3D crystal structures have been reported recently for human MDP (PDB code 1ITQ, 2.3 Å resolution) and its complex with a reversible competitive inhibitor, cilastatin (PDB code 1ITU, 1.9 Å resolution) [13,14]. The active site in each of the eight-stranded β-barrel subunits is composed of binuclear zinc ions bridged by the Glu125 side-chain located at the bottom of the barrel and cilastatin inhibitor is ideally positioned for the formation of a tetrahedral intermediate by the addition of the zinc-bound water/hydroxide [15].

Based on this structural information available, we attempted to identify MDP binding molecules and their binding modes using computational modeling methods. Theoretical approaches to the binding mode analysis have received growing attention in recent years because they

*Corresponding author. Tel.: + 82-31-728-0443. Fax: + 82-31-728-0444. Email: shchoi@insilicotech.co.kr

Molecular Simulation
ISSN 0892-7022 print/ISSN 1029-0435 online © 2007 Taylor & Francis
http://www.tandf.co.uk/journals
DOI: 10.1080/08927020701236763

can provide fast and reliable ways to pre-select compound structures for synthesis and biological studies and as a result, to reduce the cost of experimental testing especially in the early stage of drug discovery. In this article, we report the detailed results of binding mode analysis of MDP substrates using pharmacophore-based virtual screening of a large compound database and forcefield-based molecular docking studies. Various types of pharmacophore models were generated and used to screen a large virtual library including known substrates of MDP. In addition, a molecular docking study was carried out in an attempt to obtain structural insight into the MDP substrate binding mode.

2. Materials and methods

All molecular modeling work was performed on Catalyst™ 4.11 [16] for pharmacophore generation and virtual library manipulation and on Parallel LigandFit™ [17] of Discovery Studio™ 1.5 [18] for docking and scoring.

2.1 Preparation of 3D virtual library

We selected six distinct compounds from known MDP substrates and inhibitors to be used as probes in the pharmacophore-based virtual screening and high-throughput docking study. The selected compounds are structurally diverse and contain a single amide bond, which can be cleaved by MDP. Previous studies showed that a tetrahedral intermediate is formed by addition of the zinc-bound water/hydroxide as a nucleophilic reagent that attacks the carbonyl carbon atom of the scissile peptide bond [13–15]. Including cilastatin inhibitor and two other compounds with a truncated side chain, all nine compounds in the substrate and inhibitor set have molecular weights in the range of 100 ~ 300 (table 1). As the negative control set, 15,659 unique compounds were selected within the same molecular weight range from world drug index (WDI).

Conformer generation for each molecule was performed using the FAST mode option (catConf module in Catalyst) with an energy threshold of 20 kcal/mol (relative to the lowest energy conformer) and a maximum of 250 conformers. A recent study by Langer *et al.* [19] has shown that Catalyst FAST conformer model generation is appropriate for finding "bioactive" conformers most of the time. Ultimately, 3D virtual library screening was carried out using these 15,668 compounds (15,659 inactive compounds as the negative control set, nine active compounds as the positive control set).

2.2 Pharmacophore-based virtual screening

A pharmacophore (hypothesis) model consists of a 3D configuration of chemical functions surrounded by tolerance spheres. A tolerance sphere defines the volume in space that should be occupied by a specific type of chemical functionality. We constructed two types of pharmacophore models in this work; one was the manual pharmacophore-based on the X-ray crystallographic structures and the other was the automatic pharmacophore-based on the chemical structures of known ligands.

Manual pharmacophore models were generated using the structure of cilastatin complexed with MDP (1ITU). The key interactions between cilastatin and MDP are characterized by the following hydrogen bond network; the oxygen atom of the carboxyl group to the side chains of Arg230 and Tyr255, the hydrogen atom of the carboxyl group to the side chain of Asp288, the hydrogen atom of the amide group to the oxygen atom of Gly291 and the oxygen atom of the amide group to the side chain of His152 (figure 1). Based on the observed ligand–protein interactions, our pharmacophore hypotheses were constructed including three to four hydrogen bond acceptor (HBA) and hydrogen bond donor (HBD) features. Information on the size and shape of the MDP binding site was also included into the models using a set of excluded volume spheres.

Additionally, we constructed hypothetical 3D ligand-based pharmacophore models using the common feature hypothesis generation approach (HipHop) implemented in the Catalyst. Briefly, the HipHop algorithm aligns various conformers of a set of highly active compounds to generate common feature pharmacophores, which represent the essential 3D arrangement of functional groups common to a set of molecules interacting with a specific biological target. After initial energy minimization, conformational models were generated for the MDP substrates (except cilastatin with its MDP-bound active structure available). The number of conformers for each molecule was limited to a maximum of 250. Based on the conformational models, common feature hypotheses were generated consisting of pharmacophore features like HBA, HBD and hydrophobic features.

2.3 Molecular docking based on receptor structure

We also carried out molecular docking calculations using LigandFit of Discovery Studio 1.5. The docking procedure started with the generation of random conformations using a Monte Carlo based algorithm to sample the conformational space. During the docking process, the shape of a given conformation (defined by the principal axes of moment inertia) was compared with the shape of the active site. Rigid body minimization of the candidate ligand poses was performed in two stages. The first optimization was done immediately after a ligand with a randomly altered conformation had been positioned in the active site after a shape alignment. This first optimization employed a steepest descent algorithm. The second optimization using the Broyden–Fletcher–Goldfarb–Shanno minimizer [20,21] was performed on the selected configuration. Next, the *in situ* minimization of ligand conformation was performed to minimize both the ligand internal energy and

Table 1. Chemical structures of known MDP substrates and inhibitors.

Ligand name	*Compound ID*	*Reference*	*PDB code*
Truncated cilastatin	1	[15]	1ITU
Cilastatin	2	[15,30]	
LTD-4	3	[15,30]	
Truncated imipenem	4	[15]	
Imipenem	5	[15,30]	
Gly–D-Asp	6	[32]	
Gly–D-Ala	7	[31,32]	
Gly–D-Phe	8	[15,30]	
Cys–Gly	9	[3,14]	

Ligand structures

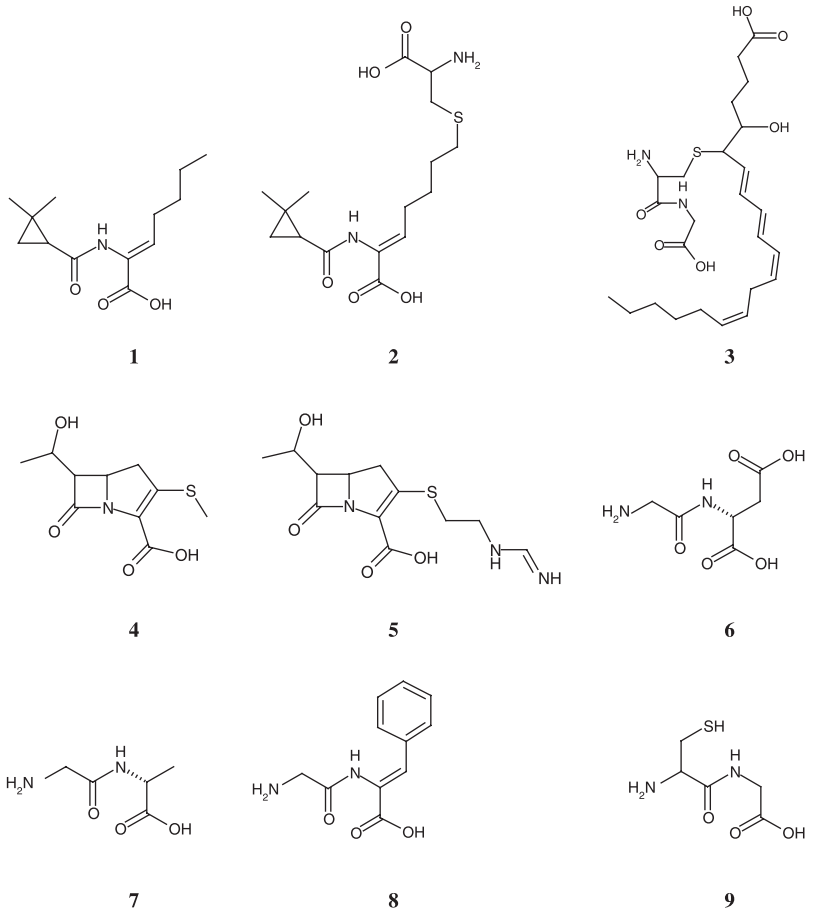

the ligand–receptor interaction energy while holding the receptor atom coordinates fixed.

Several docking simulations were performed to reproduce the experimentally observed binding mode of cilastatin ligand and to identify MDP substrates from a compound library. In order to construct the receptor structure for docking simulation, all hydrogen atoms were added to the protein crystal structure 1ITU and two zinc atoms and the zinc-bound water molecule (Wat421) were incorporated.

First, manual docking was performed for 20 conformers of cilastatin. The docking site was searched based on the shape of the protein using the eraser and flood-filling algorithm [22,23]. The ligand-accessible grid was defined such that the minimum distance between the grid point and the protein was 2.0 Å for hydrogen atoms and 2.5 Å for heavy atoms and the grid resolution was 0.5 Å with a site opening parameter of 10 Å. The grid was set to extend 3 Å beyond the defined active site in all directions and used to calculate the non-bonded interaction between all the atoms of ligand and protein residues using the consistent force field potential function [24,25]. The non-bonded cutoff was set to 10 Å and electrostatic interactions were calculated using a distance-dependent dielectric constant. The top 10 cilastatin conformers with different docking scores or root-mean-square displacement (RMSD) values were saved for the further analysis.

Next, we docked and scored nine active and 15,659 decoy compounds to the target protein using parallel LigandFit docking program. This high-throughput docking

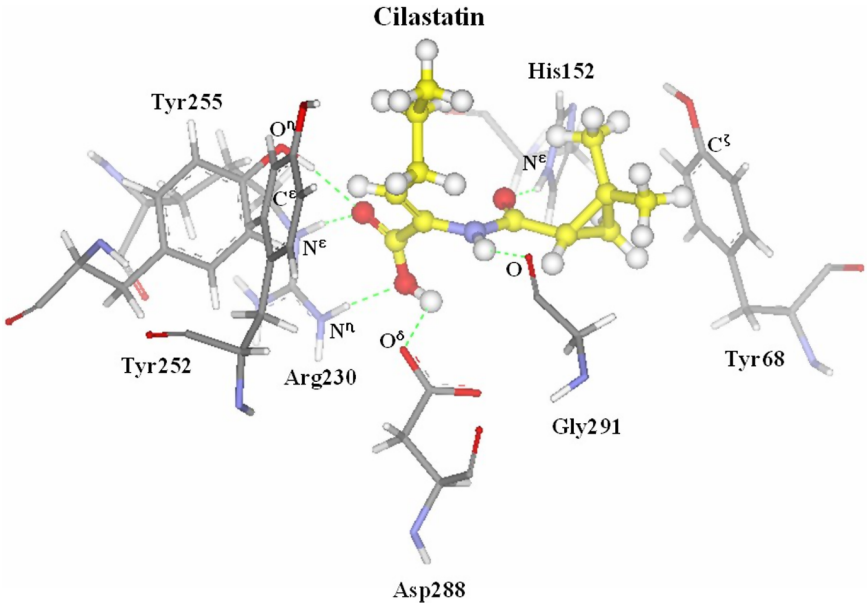

Figure 1. MDP interactions between the cilastatin molecule and the residues comprising the active site. The cilastatin ligand is shown in ball-and-stick style with carbon atoms in yellow, oxygen atoms in red and nitrogen atom in blue. The hydrogen bonding are monitored in green (colour in online version).

procedure was, in effect, identical with the previously mentioned manual docking of cilastatin in every step except a few. Highly scored 20 ligand conformations were archived based on 10 scoring functions of Dock, Ligscore1, Ligscore2, LUDI1, LUDI2, LUDI3, PMF, PLP1, PLP2 and JAIN scores [26–28].

3. Results and discussions

In order to compare the accuracy and performance between pharmacophore-based virtual screening and molecular docking for this MDP system, we performed both pharmacophore hypothesis approach and receptor-based semi-flexible docking simulation. Hypothesis generation and binding site search were guided based on previous experimental results and the crystal structure of MDP.

A previous mutagenesis study [29] indicated that His152 is involved in the enzyme catalysis and plays an important role in substrate/inhibitor binding. The dimethylcyclopropyl group and the alkyl end group of cilastatin are surrounded by Tyr68 and Tyr252 and both ends of the cilastatin moiety are clamped tightly by the hydrophobic sidewalls, while all other substrates lack a group to buttress at its terminus. Cleavage of the cilastatin amide bond is prevented due to the dimethylcyclopropyl and alkyl end groups and it is the reason why cilastatin works as an inhibitor, not a substrate [14,15]. Our investigation was focused on this scissile peptide bond.

3.1 Pharmacophore-based virtual screening

The starting point for the hypothesis generation process was the PDB entry 1ITU detected at a resolution of 1.9 Å, which contains MDP in complex with cilastatin inhibitor. Although cilastatin contains three HBAs and two HBDs, the hypotheses assuming the hydroxyl group of the carboxyl terminus as a HBD could not retrieve all the MDP substrates from our virtual library. Therefore, we excluded this HBD feature from hypothesis generation and generated five pharmacophore models (figure 2) consisting of three HBA and one HBD features. These pharmacophore models were used as the query tool in pharmacophore-based virtual screening of large compound databases to ensure the selectivity of the model and identify essential features of MDP binding.

Herein, we introduced enrichment ratio (E) and yield ($\%Y$) to evaluate the quality of a hit list as formulated in equations (1) and (2), respectively:

$$E = \frac{\frac{H_a}{H_t}}{\frac{A}{D}} = \frac{H_a \times D}{H_t \times A} \quad (1)$$

$$\%Y = \frac{H_a}{H_t} \times 100 \quad (2)$$

where, H_t is the total number of compounds in the hit list, H_a is the number of known actives in the hit list, A is the number of active compounds in the database and D is the number of compounds in the database. Enrichment ratio is calculated as the ratio of the yield of actives in the hit list relative to the yield of actives in the database. This ratio is an index of the increase in the proportion of hits found in any given sample of compounds, compared with the proportion expected from a random sample. Yield ($\%Y$) is the percentage of known actives in the hit list.

Table 2 shows the performance of the different hypotheses in the virtual screening. The best pharmacophore hypo1 in terms of yield and enrichment ratio retrieved 1,230 hits including six out of nine actives and

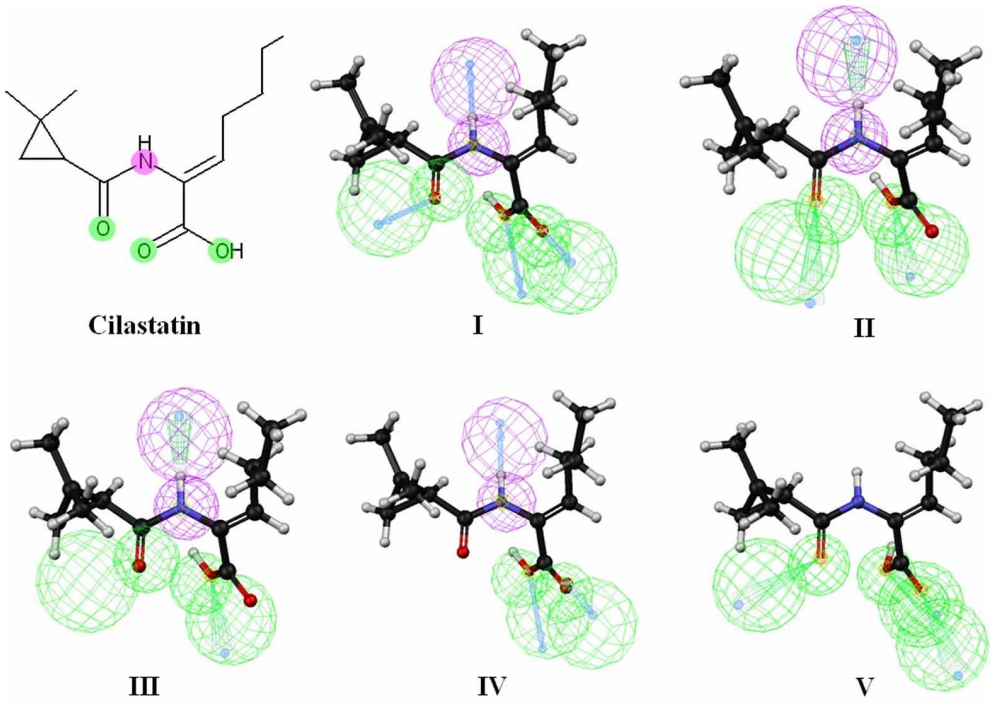

Figure 2. The hypotheses for cilastatin inhibitor. The colored spheres correspond to the pharmacophoric features in both 3D and 2D representations with the following colors: green, HBA; magenta, HBD.

achieved enrichment ratio of 8.5. Other queries retrieved so many compounds from the virtual library that the enrichment of active compounds was not significant.

In order to compare the hitting performance of our approaches by hypo1 and random search, hits were ranked according to their fit values. The calculation was performed to determine how well a compound fits a particular hypothesis, i.e. how well the ideal locations of the features can be matched by the corresponding functional groups of a molecule. The enrichment plot for 1,230 hit compounds based on the fit value was represented in figure 3. The enrichment plot illustrates how fast all the MDP substrates could be identified if the compounds are resorted according to the fit value. An enrichment curve close to the perfect model is a good indication of the high prioritization power of the hypothesis. Based on this enrichment curve, we found that our pharmacophore model was much more efficient than random search; the top 532 hits (4.4% out of 15,668 compounds) contained six of the known actives (67% out of nine known substrates) in our approach.

Although the enrichment by our pharmacophore-based approach was significant, the efficiency was not remarkable. This low efficiency could probably be explained by the fact that our cilastatin pharmacophores contained only HBD and HBA features; more specific features like hydrophobic (aliphatic and aromatic) and ionizable (positive and negative) groups were not included. The hydrogen bonding features were localized only at the center of molecule, which also lowered the structural diversity of the pharmacophore model.

To verify the manual pharmacophore-based on MDP-bound cilastatin structure, we also constructed a common feature pharmacophore model based on nine known MDP substrates using HipHop algorithm of Catalyst. The features consist of generalized chemical functions that simulate those characteristics necessary for receptor binding. The common feature pharmacophore model was in reasonable agreement with the manual pharmacophore hypo1. The HipHop hypothesis consists of three HBA and one HBD features showing a good overlap with known MDP substrates and does not include more specific

Table 2. Calculation results on pharmacophore-based virtual screening.

Hypothesis no.	*Number of actives*	*Total retrieved*	*Yield (%)*	*Enrichment*
Database	*9*	*15,668*	*0.057*	*1.000*
I	6	1,230	0.488	8.492
II	8	3,769	0.212	3.695
III	9	2,893	0.311	5.416
IV	8	3,420	0.234	4.072
V	8	3,422	0.234	4.070

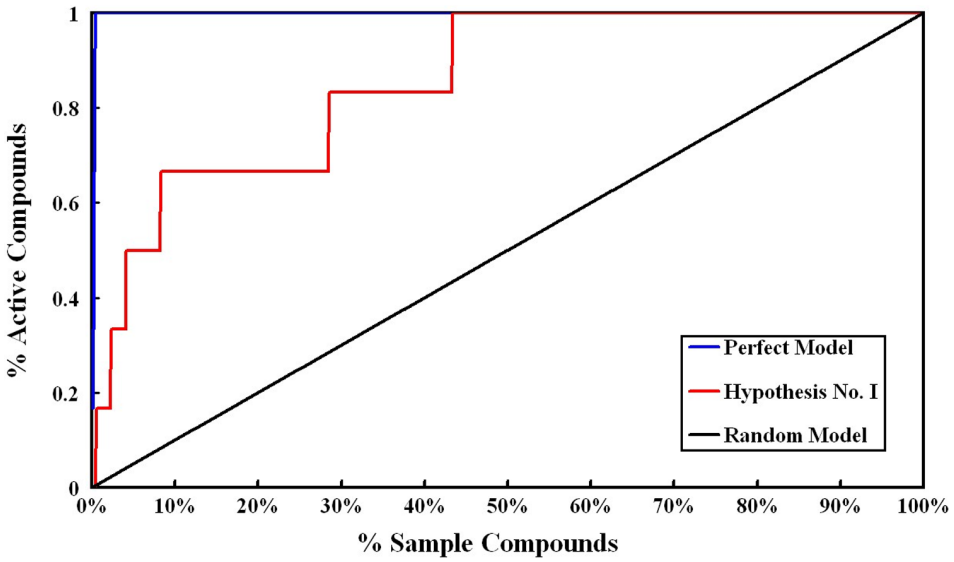

Figure 3. Enrichment plot of the percent active found versus percent of the fit value ordered list screened, using hypothesis no.1. The black line represents the values expected if actives were selected at random. The blue line represents the values expected if all active are placed sequentially at the top of the list.

features like hydrophobic (aliphatic and aromatic) and ionizable (positive and negative) groups (figure 4(a)). The overlap between HipHop hypothesis and hypo1 pharmacophore (figure 4(b)) shows that the orientations of the features are similar in the two pharmacophores with a RMSD of 1.52 Å.

Our hypothesis (hypo1) produced rather reliable validation results in the virtual screening processes, returning selective hit lists from the virtual library containing MDP substrates. Three HBA and one HBD pharmacophore features were successfully identified, illustrating the important interactions between MDP and its substrates.

3.2 *Molecular docking based on receptor structure*

Molecular docking involves forcefield-based atomic simulation and is more sophisticated than pharmacophore-based screening. General molecular docking considers the conformational flexibility of ligand and receptor; however the computational cost is significant. In this work, we performed the semiflexible molecular

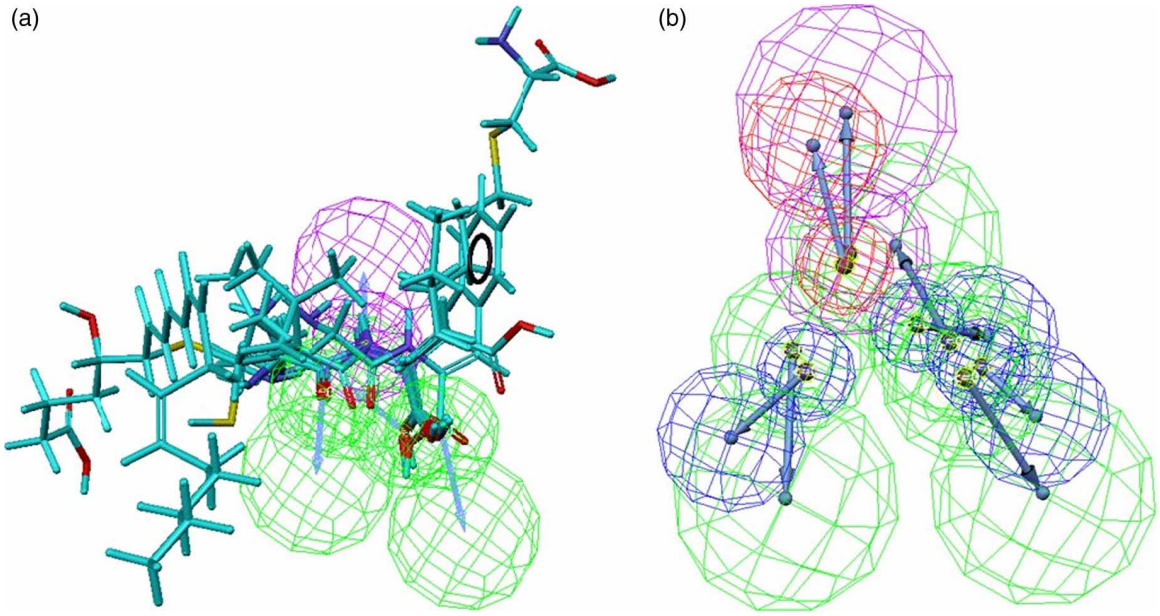

Figure 4. (a) The HipHop pharmacophore consists of three HBA features (green) and one HBD (magenta) feature. The common feature model is generated based on known active substrates for MDP and consistent with the features of manual hypothesis. (b) Overlays between the hypothesis from HipHop and hypo1 pharmacophore with the following colors: HBD (green) and HBA (magenta) for HipHop pharmacophore and HBD (blue) and HBA (red) for hypo1 pharmacophore (colour in online version).

Table 3. Calculation Results on cilastatin docking to MDP.

Binding Group		*Binding Feature*			
Ligand functional group	*Protein residue*	*Experiment Crystal ligand*	*Docking Simulation*		
			Crystal rigid[†] *Crystal water*	*Conformer flexible*[‡] *Crystal water*	*Conformer flexible Without water*
Carboxyl group (—COOH)	Arg230 $N^{\varepsilon}H$, $N^{\eta}H$	H-bond	H-bond	H-bond	H-bond
	Tyr255 $O^{\eta}H$	H-bond	H-bond	H-bond	–
	Asp288 O^{δ}	H-bond	–	–	–
Amide hydrogen (—NH)	Gly291 O	H-bond	H-bond	H-bond	H-bond
Amide oxygen (—C═O)	His152 $N^{\varepsilon}H$	H-bond	H-bond	H-bond	–
Cyclopropyl group	Tyr068 C^{ζ}	3.52 Å	3.65 Å	3.47 Å	3.29 Å
Alkyl endgroup	Tyr252 C^{ε}	3.90 Å	3.85 Å	3.79 Å	4.94 Å
Carbon atom of —C═O	Water421	2.82 Å	2.45 Å	2.73 Å	–
RMSD (Å)		0.00 Å	0.44 Å	0.37 Å	1.55 Å

[†] In rigid docking, only the position and the orientation of the crystallographically determined cilastatin structure are altered to find optimized docking structure. [‡] The torsion angles of the cilastatin are randomly varied during docking and a Monte Carlo method is employed in the conformational search of the ligand.

docking simulation to save computational time. During the process of semiflexible docking, the flexibility of ligand is fully considered while the interaction with receptor is calculated using the grid potentials predetermined from the molecular field of the fixed receptor structure.

At first, the cilastatin inhibitor was re-docked to the corresponding MDP crystal structure to validate the LigandFit program for its docking accuracy and reliability to reproduce the binding geometry of cilastatin. Herein, crystal rigid docking utilized the single conformer of cilastatin taken from the MDP bound crystallographic structure, while conformer flexible docking utilized the various conformers randomly generated, as represented in table 3. The accuracy of a pose was assessed in two ways. First, RMSD of cilastatin heavy atoms from the crystal structure was calculated. Second, the predicted pose was compared to the experimentally observed one regarding the presence of key interactions with MDP. The difference in RMSD is very small between the docked and crystallized structures, 0.44 Å for crystal rigid docking and 0.37 Å for conformer flexible docking, respectively. Most of the key hydrogen bonding interactions observed in the crystal structure were accurately reproduced in the docking results, except the interaction between the cilastatin carboxyl group and Asp288 (table 3).

Furthermore, we tried to identify the role of a crystallographically observed water molecule in the interaction between MDP and cilastatin. According to recent studies, the water molecule (Wat421) in the MDP active site could be activated by Asp288 on the negatively charged sidewall [13–15]. The deprotonated Wat421 would acts as a nucleophile to attack the carbonyl carbon atom of the scissile peptide bond and to form a tetrahedral intermediate. The docking study without the crystallographically bound water produced poor docking results; RMSD of cilastatin in the active site was 1.55 Å and only two hydrogen bonding interactions for residue Arg230 and Gly291 were reproduced. Based on these results, it could be concluded that Wat421 plays an important role in the ligand–receptor interaction and there is a good agreement between the results of simulations and the previous experimental data [13–15].

Finally, nine known active and 15,659 decoy compounds were docked flexibly into MDP and scored

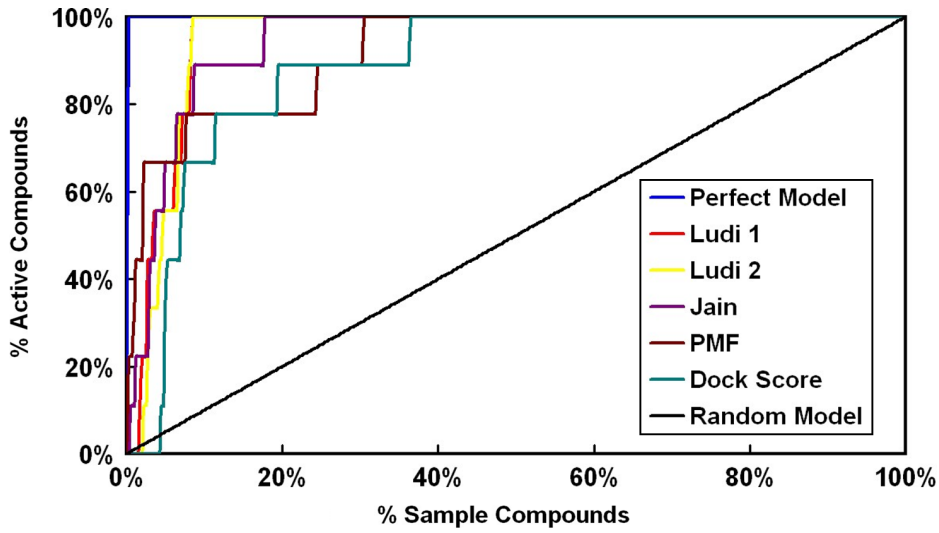

Figure 5. Number of actives plotted against ligand rank corresponding to distinct scoring functions in the virtual library.

to determine appropriate scoring functions. Ten scoring functions (Dock, Ligscore1, Ligscore2, Ludi1, Ludi2, Ludi3, PMF, PLP1, PLP2 and JAIN) were evaluated for their predictability and figure 5 shows the number of actives plotted against the ligand rank corresponding to distinct scoring functions. Ludi1, Ludi2, JAIN, PMF and Dock functions provided good scoring results with respect to the enrichment plot of the library and especially Ludi1 and Ludi2 scoring functions ranked all the active compounds within the top 10% (1,567 compounds) scoring compounds. JAIN, PMF and Dock scoring functions extracted six out of nine active compounds within the top 10% of the hit list. LigScore1 and PLP2 scoring functions identified at least 50% of the active compounds in the top 20% of the entire database.

Based on this semiflexible docking simulation on MDP, we found that the virtual screening with proper scoring functions could be used for the proximate docking and ranking of compounds with putative MDP binding potency to discriminate between the actives and inactives. Higher enrichment values were obtained using the molecular docking than the pharmacophore screening method.

4. Conclusion

We performed virtual screening on MDP using an automated ligand-based approach (pharmacophore) and a structure-based approach (molecular docking). While the cilastatin-based pharmacophore models consisting of three HBA and one HBD features could be used to retrieve the actives from the virtual library successfully, the enrichment process was not highly selective and many false positive compounds were also mapped together into the hypothesis. In the molecular docking studies, however, the crystallographically observed binding geometry of cilastatin was reproduced precisely and the high-throughput docking successfully produced the selective hit list from the 3D database containing MDP substrates. We could also characterize the role of the crystal water in the interaction between cilastatin and MDP. In general, the structure-based approach produced better results than the ligand-based approach for correct identification of the MDP substrate-binding mode. The virtual screening method developed through this modeling study could serve as a fast and reliable pre-selection filter to speed up the search for potential MDP substances.

Acknowledgements

This work was supported by a grant (Code: 20050401034696) from BioGreen 21 Program, Rural Development Administration, Republic of Korea. We thank Accelrys Korea for the support of modeling software.

References

[1] S. Keynan, N.M. Hooper, A.J. Turner. *Zinc Metalloproteases in Health and Disease*, Taylor & Francis, London (1996).
[2] I.J. White, J. Lawson, C.H. Williams, N.M. Hooper. This enzyme is also referred to as leukotriene-D4 hydrolase. *Anal. Biochem.*, **268**, 245 (1999).
[3] D. Rajotte, E.J. Ruoslahti. Membrane dipeptidase is the receptor for a lung-targeting peptide identified by *in vivo* phage display. *J. Biol. Chem.*, **274**, 11593 (1999).
[4] B.J. Campbell. Renal dipeptidase. *Methods Enzymol.*, **19**, 722 (1970).
[5] D.J. Armstrong, S.K. Mukhopadhyay, B.J. Campbell. Physico-chemical characterization of renal dipeptidase. *Biochemistry*, **13**, 1745 (1974).
[6] H. Kropp, J.G. Sundelof, R. Hajdu, F.M. Kahan. The tight binding and reversibility features have allowed cilastatin to be exploited in purification of MDP by affinity chromatography. *Antimicrob. Agents Chemother.*, **22**, 62 (1982).
[7] D.W. Graham, W.T. Ashton, L. Barash, J.E. Brown, R.D. Brown, L.F. Canning, A. Chen, J.P. Springer, E.F. Rogers. Inhibition of the mammalian β-lactamase renal dipeptidase (dehydropeptidase-I) by Z-2-(acylamino)-3-substituted-propenoic acids. *J. Med. Chem.*, **30**, 1074 (1987).
[8] H. Adachi, Y. Tawaragi, C. Inuzuka, I. Kubota, M. Tsujimoto, T. Nishihara, H. Nakazato. Primary structure of human microsomal dipeptidase deduced from molecular cloning. *J. Biol. Chem.*, **265**, 3992 (1990).
[9] B.J. Campbell, Y.C. Lin, R.V. Davis, E. Ballew. The purification and properties of a particulate renal dipeptidase. *Biochim. Biophys. Acta*, **118**, 371 (1966).
[10] R. Pasqualini, E. Ruoslahti. Organ targeting *in vivo* using phage display peptide libraries. *Nature*, **380**, 364 (1996).
[11] D. Rajotte, W. Arap, M. Hagedorn, E. Koivunen, R. Pasqualini, E. Ruoslahti. Molecular heterogeneity of the vascular endothelium revealed by *in vivo* phage display. *J. Clin. Invest.*, **102**, 430 (1998).
[12] W. Arap, R. Pasqualini, E. Ruoslahti. Cancer treatment by targeted drug delivery to tumor vasculature in a mouse model. *Science*, **279**, 377 (1998).
[13] Y. Nitanai, Y. Satow, H. Adachi, M. Tsujimoto. Crystallization and preliminary X-ray investigation of a glycoprotein, human renal dipeptidase. *J. Cryst. Growth*, **168**, 280 (1996).
[14] Y. Nitanai, Y. Satow, H. Adachi, M. Tsujimoto. Crystal structure of human renal dipeptidase involved in β-lactam hydrolysis. *J. Mol. Biol.*, **321**, 177 (2002).
[15] T.P. Smyth, J.G. Wall, Y. Nitanai. A substrate variant as a high-affinity, reversible inhibitor: insight from the X-ray structure of cilastatin bound to membrane dipeptidase. *Bioorg. Med. Chem.*, **11**, 991 (2003).
[16] Catalyst, Version 4.11, Accelrys, Inc., San Diego (2005).
[17] C.M. Venkatachalam, X. Jiang, T. Oldfield, M. Waldman. LigandFit: a novel method for the shape-directed rapid docking of ligands to protein active sites. *J. Mol. Graph. Model.*, **21**, 289 (2003).
[18] Discovery Studio, Version 1.5, Accelrys, Inc., San Diego (2006).
[19] J. Kirchmair, C. Laggner, G. Wolber, T. Langer. Comparative analysis of protein-bound ligand conformations with respect to catalyst's conformational space subsampling algorithms. *J. Chem. Inf. Model.*, **45**, 422 (2005).
[20] D. Goldfarb. A family of variable-metric methods derived by variational means. *Math. Comput.*, **24**, 23 (1970).
[21] C.G. Broyden. The convergence of a class of double-rank minimization algorithms: 2. The new algorithm. *J. Inst. Math. Appl.*, **6**, 222 (1970).
[22] J.D. Foley, A. Van Dam. Fundamentals of interactive computer graphics, Addison-Wesley, MA (1982).
[23] D.F. Rogers. Procedural elements for computer graphics, McGraw-Hill, New York (1985).
[24] K. Baldridge, R. Fine, A. Hagler. The effects of solvent screening in quantum mechanical calculations in protein systems. *J. Comput. Chem.*, **15**, 1217 (1994).
[25] M. Waldman, A.T. Hagler. New combining rules for rare gas van der Waals parameters. *J. Comput. Chem.*, **14**, 1077 (2003).
[26] A. Krammer, P.D. Kirchhoff, X. Jiang, C.M. Venkatachalam, M. Waldman. LigScore: a novel scoring function for predicting binding affinities. *J. Mol. Graph. Model.*, **23**, 395 (2005).

[27] I. Muegge, Y.C. Martin. A general and fast scoring function for protein–ligand interactions: a simplified potential approach. *J. Med. Chem.*, **42**, 791 (1999).

[28] H.J. Böhm. The development of a simple empirical scoring function to estimate the binding constant for a protein–ligand complex of known three-dimensional structure. *J. Comput. Aided Mol. Des.*, **8**, 243 (1994).

[29] S. Keynan, N.M. Hooper, A.J. Turner. Directed mutagenesis of pig renal membrane dipeptidase His219 is critical but DHXXH motif is no essential for zinc binding or catalytic activity. *FEBS Lett.*, **349**, 50 (1994).

[30] T.P. Smyth. Substrate variants versus transition state analogues as noncovalent reversible enzyme inhibitors. *Bioorg. Med. Chem.*, **12**, 4081 (2004).

[31] Y. Kera, Z. Liu, T. Matsumoto, Y. Sorimachi, H. Nagasaki, R. Yamada. Rat and human membrane dipeptidase: tissue distribution and developmental changes. *Comp. Biochem. Phys. B*, **123**, 53 (1999).

[32] T. Watanabe, Y. Kera, T. Matsumoto, R. Yamada. Purification and kinetic properties of a D-amino-acid peptide hydrolyzing enzyme from pig kidney cortex and its tentative identification with renal membrane dipeptidase. *Biochim. Biophys. Acta*, **1298**, 109 (1996).